VOL. 4, NO. 3, MAY 2009 ISSN 1819-6608
ARPN Journal of Engineering and Applied Sciences


www.arpnjournals.com

LATERAL STABILITY OF RAIL VEHICLES- A COMPARATIVE STUDY

M. Messouci
Université M'Hamed Bougara, département de mécanique, FHC, Boumerdès. Algeria
E-Mail: messouci_ma15@yahoo.fr

ABSTRACT

In this study, a linear analysis is developed to evaluate the critical speed for a rail vehicle when wheels with controlled creep forces are used. We show the effect of varying the primary and secondary suspension parameters and varying a few others such as the effective conicity, the masses and the torsional-damping coefficient between wheels. We show that critical speeds at which the instability occurs can be increased beyond the actual operating speed by proper selection of design parameters. We show in particular the interest of a yaw stiffness provided between the car body and each bogie frame in conjunction with a primary suspension system having springs with relatively lower longitudinal stiffness a feature that allows good curving performance. The behaviour of the vehicle is considered in comparison with that of a conventional one having, rigid wheel sets or free wheels turning on the same axle independently of each other.

Keywords: lateral stability, primary and secondary suspension, critical speed, torsional damping coefficients.

1. Foreword

A progress without cease and more and more rapidly in the range of speeds by offering improved performance is a permanent objective of the rail administrations. The growth in speed is not without asking traction engineers to search for the difficult compromise between good stability performance and good curving performance in low radius curved tract minimising wear of tread, flanges and rail [1]. Indeed, with a conventional vehicle, it is necessary to rein the wheel set in the bogie for a stable rolling at high speeds. However, the almost total longitudinal rigidity of the suspension between the wheel sets and the bogies is in contradiction with an easy inclusion in curves: it is an interference with regard for the wheel sets, to take up radial alignments, so that the vehicle is steered round curves. In addition, this vehicle with rigid bogies and rigid wheel sets is sensitive to changes in the wheel effective conicity resulting from surfaces wear. The speed limit from the bogie can only maintained by monitoring the wear treads wheels (profile 1/40 refreshed every 200000km) and the narrow adjustment of the yaw elastic reaction torque bogie / body, which tends to worsen a good behaviour on curves. Its effect is limited to a maximum, beyond which the increase of this secondary yaw restraint does no more benefit [2]. Moreover, such increases in speed could lead to an inevitable downgrading of the dynamic comfort of passengers [3]. The classical vehicle has a number of shortcomings and this impels the designers developing rail vehicle to seek for solutions new in principle. There is therefore, a sufficiently well grounded reason for the more complicated and costly systems.

There is then a trend in the development, which is analogue to the following "if you are using prefabricated elements, you have fewer opportunities than using bricks"

1.1 Flexible bogie

The conventional guidance flange contact being an unacceptable solution, let us split the bogie: a current interest has grown in the world in favour of flexible bogie (Scheffel design). That is the designation given to the bogie allowing the shear stiffness increase without increasing, by the way, the bending stiffness of which, as a result, led to a good entry in the curves. Another important aspect of the device in question is that for a given bending stiffness there is no additional benefit to gain beyond a certain shear stiffness value. On the other hand, there is also a minimum bending stiffness to exceed in order to obtain a permissible critical speed [4].

Moreover, as with the classic vehicle, we can effectively improve the stability by retaining the bogie by an anti-yaw device to the body. Again, there is an inability to solve effectively this unavoidable problem of bogie yaw [5].

1.2 Classic wheel set

The wheel set is a classic rigid axle with two wheels firmly fixed to it. It blames this wheel set as a source of wheels and rail working surface wear. As presented, it is not an ideal solution. Another problem inherent in this principle is the back-and-forth movement of wheels within the clearance between the wheel set and the track. These disadvantages have leaded repeatedly ideas and experiences to turn the wheels on the same axle independently of each other. The merit of the rigid wheel set is simplicity in design. The utmost simplicity of design have gained it wide acceptance nowadays.

1.3 Free wheels

The rigid wheel set is not an acceptable solution, let us split the axle. In the past, many projects have considered vehicles having free wheels. Many experiments were made and they have failed. Tests showed that the wheel rolls in permanent contact with the rail edge. There is no trend for such mechanism to take off from the path [6]. Only other variants of assembling these wheels are likely to lead to the elimination or reduction of the disadvantage cited above. The free wheels may not take rail direction spontaneously. There is a need of an outside influence or guidance (bilateral contact) or angular

direction. An author has presented a number of possible variants [7]. It also appears that the fitting of free wheels on an axle, according to the results presented in this study, is not likely to improve the behaviour of rail vehicles with a soft longitudinal stiffness of the primary suspension. It shows that we can get good results with both an anti-yaw damper connecting the body to the bogies and a mean value of the primary suspension longitudinal stiffness.

1.4 Wheel set with controlled creep forces

It consists of two wheels rigidly linked to two semi hollow shafts turning around an inner common axle. A torsional damper connects the two half-hollow shafts. The action of the coupled wheels on one another is a viscous friction type. The relative rotation between wheels will be more or less constrained depending on the coefficient of resistance value or damping coefficient C_φ of the torsional damper. This consolidation provides an opportunity to the mechanism to return to its equilibrium position: the wheel that climbs up the flange taking the advance on the other wheel causes a rotation of the axle, which tends to bring it to the central position in the track [8]. This constructive feature gives us, in fact, the ability to control the creep forces magnitude generated at the wheels. It reveals new opportunities and at the same time justifies an old necessity: New opportunities in the sense it achieves increase in traffic speed on conventional lines to the point that the yaw elastic reaction torque between body and the bogies is rendered superfluous. We realise that operational speeds of 400 or 500km.h^{-1} are possible with a soft primary suspension allowing the wheel sets to take up approximately radial alignments in curved track. A former necessity, in the sense that the classical wheel set cannot be evicted when it comes to steer the vehicle around the track with a great curvature. There is therefore a need to lock up during motion the link between the wheels under a certain value of radius of the track achieving a correct alignment of the wheel sets, an adequate sizing of the damper and a reliability objective.

2. INTRODUCTION

In this study, we examine the possibility for a rail vehicle having wheel sets with controlled creep forces to satisfy the contradictory requirements between good stability performance and good curving performance. The behaviour of a vehicle equipped with such wheel sets is considered in comparison with that of a conventional vehicle having rigid wheel sets or free wheels. There is a problem of assessing the stability in the small. We will determine the critical speed of a vehicle as a whole moving at a constant speed along track alignment and without defects, according to different construction parameters. The critical speed is the limit of safety motion where instability is either unsustainable or frankly destructive. The complexity arising from the number of degrees of freedom confines this study to a numerical analysis and discussion.

In strictly speaking, such a study is very difficult because the vehicle as a dynamic system has a large number of degrees of freedom and several non-linearity whose main comes from the wheels tread profile, the contact actions laws rail/wheel and the damping of the suspension. However, the linearization can address this problem to obtain guidance, at least qualitatively, assessing the degree of quality of the dynamic system configuring the vehicle subject to review.

3. VEHICLE ARCHITECTURE

The vehicle used consists of a body, two identical bogies and four wheel-axles sets. Figure-1 depicts a scheme of one bogie surrounded by the provision of suspension.

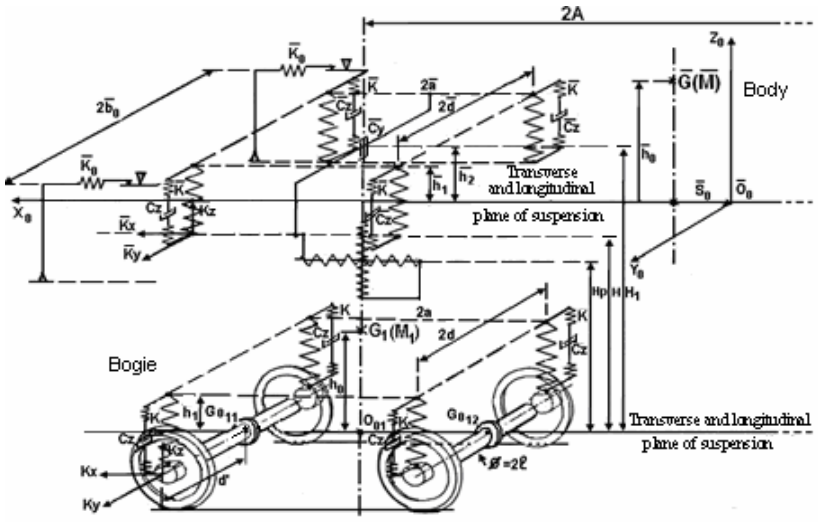

Fig.1. Layout of the suspensions elements of a four wheeled-rail vehicle and its principal parts.

The primary suspension between the bogies and the wheel sets is made by weightless springs in series with rubber pads to cut the transmission of noise. Four dampers in parallel with springs complement the suspension. The same goes for the secondary suspension. The body/bogie coupling link allows to the body to perform an oscillatory

motion around a cylindrical and longitudinal hinge placed underneath. The lowest end of this coupling link slides in a ball-and socket joint judiciously located in the bogie frame. To control the movement of the bogie under the body, we introduce an anti-yaw damper "KONI" type whose nonlinear operation was apprehended by the first harmonic method [2]. It is also shown that the angular rigidity of the system for hanging these anti-yaw dampers determines the maximum critical speed that can be obtained for given bogie characteristics. Therefore, these dampers will be regarded as passive in this study. The expression of anti-yaw elastic torque being: $C(\alpha_k) = 2\bar{K}_0\bar{b}_0^2\alpha_k$ [2]. (1)

3.1 Key assumptions

The solids of the vehicle, as well as the tracks are supposed rigid absolutely. The rail alignment supposedly perfect with constant gauge, is located in a horizontal plane. All the displacements are assumed small. The vehicle is supposed to move at a constant speed. We believe that the rubbing body/bogie coupling link is zero and can be disregarded. The rubbing against the yaw brings some damping. The system is characterized by elastic rigidities in three directions. The springs and viscous dampers are supposed to have linear characteristics.

For purpose of comparison vehicles, the specifications of the wheel sets are not changed. Therefore, we assume the same masse distribution.

The centres of gravity of the body and the bogies are located in a median and longitudinal plane. The bogies have a dual transverse and longitudinal symmetry. The longitudinal symmetry of inertia, elasticity and sensitive linear phenomena can decouple the vertical actions from the transverse ones.

4. MATHEMATICAL FORMULATION

In this study, a mathematical model is developed to calculate the complex eigenvalues of a characteristic equation as a function of vehicle speed. The characteristic equation is derived from linear equations of motion of the vehicle. A computer program has been written to assess the influence of primary and secondary suspension, masses and damping in rotation between the wheels on the lateral stability of the vehicle. The lateral stability characteristics of the rail vehicle are assessed from maximum (critical) speeds of motion in the straight line. The successive steps that allow for the construction of the differential equations are as follows: writing of potential, kinetic and dissipative energy put into play during the movement. Finally, writing the differential system.

4.1 Bases definition

The description of the movement is made in a right-handed coordinate $\bar{O}_o;x_o,y_o,z_o$ system moving with a uniform rectilinear speed (advance speed of the vehicle) toward the $\bar{O}_o x_o$ - axis relative to Galilean benchmark $\bar{O}_g;x_g,y_g,z_g$ tied to the track and direct of which the $\bar{O}_g x_g$ -axe points along the rail. The reference coordinate system $\bar{O}_o;x_o,y_o,z_o$ will be considered Galilean as well. In the absence of parasitic movements the $\bar{O}_g x_g$ -axis coincides with the vehicle roll axis. The plane containing the axis of the roll is called plane of suspension. It is located halfway up strings.

We define the mobile frame $\bar{O}_c;x,y,z$ linked to the body. Its origin $\bar{O}_c$ is located at the intersection of transverse and longitudinal plane of suspension and the vertical passing through the geometric centre base body. It is the elastic forces centre. At a state of rest, the centre $\bar{O}_c$ coincides with the origin $\bar{O}_o$. The mobile frames $O_k;x,y,z$ are attached to the bogies centres O_k located at the intersection of the common horizontal plane passing halfway up strings of the primary suspension and the vertical lines passing through the geometric centre of each base bogie.

4.2 Vehicle configuration (coordinates)

4.2.1 Body configuration

We will denote $\bar{G}$ the inertia centre of the body that we consider as a solid. The angles defining the orientation of the mobile system axis with respect to the fixed ones are the yaw $\bar{\alpha}$, the roll (rocking) $\bar{\theta}$ and the pitch (galloping) $\bar{\varphi}$. Moreover, the mobile base is identified to the solid itself. It should be added three degrees of freedom of translational motion: the swing $\bar{y}$, the rebounding (jumping) $\bar{z}$ and the advance $\bar{x}$.

4.2.2 Bogies configuration

We will denote G_k the bogies centre of inertia that we consider being a solid designated by (C_k). The angles defining the orientation of axes of mobile system in relation to fixed axes are the yaw α_k, the roll θ_k and the pitch φ_k. Moreover, the mobile base x_k, y_k, z_k is identified to the solid itself. It should be added three degrees of freedom of translational motion: the swing y_k, the rebounding z_k and the advance z_k.

4.2.3 Wheel sets configuration

We will denote G_{ki} the centre of inertia for each wheel set that we consider being a solid designated by (S_{ki}).

The yaw α_{ki} and the roll ψ_{ki} characterize the angular position of the mobile frame with respect to a fixed one. The wheels angular rotational motions are around $G_{s_{11}} y_{ki}$ - axis of the mobile frame $G_{ki};x_{ki},y_{ki},z_{ki}$ attached to the solid S_{ki}.

Kinematics relations bind the roll angle ψ_{ki} to the swing y_{ki}. The motion is studied from geometric standpoint in [9]:

$$\psi_{ki} = \Gamma y_{ki} \text{ With } \Gamma = \frac{\gamma_0}{e_0 - r_0\gamma_0} \quad (2a, b)$$

In addition, the vertical position of the wheel set inertia centre is given by the geometry study:

$$z_{ki} = f(y_{ki}, \alpha_{ki}) \text{ Or } z_{ki} = \xi \frac{y_{ki}^2}{2} - \varepsilon_0\gamma_0 \frac{\alpha_{ki}^2}{2} \quad (3)$$

With

$$\xi = \frac{1}{R - R'}\left\{\frac{e_0 - R\gamma_0}{e_0 - r_0\gamma_0}\right\}; \varepsilon_0 = e_0 - (R - 2r_0)\gamma_0 \quad (4a, b)$$

It should be added three degrees of freedom of translational motion: the swing y_{ki}, the rebounding z_{ki} the advance x_{ki} and the increment angle in rotation φ_{kij}.

4.3 Equations of motion

The system of 38 differential equations simulating the dynamic behaviour of the vehicle is divided into two complementary independent groups: the first, not related to this study comprises 13 equations. It characterizes the vertical and longitudinal dynamics. It concerns the following variables: x: advance, z: rebound, φ: pitching.

The second comprises 25 equations and characterizes the transverse dynamic with the following variables:

y: swing, θ: rolling, α: yaw.

This decoupling of great importance for theoretical studies and experimental testing is a consequence of the significant linear phenomena and the symmetry of the various solids of the vehicle.

Relative displacements between the body and the bogies are

$$\{\bar{U}_k\} = [T_c]\{U^c\} - [T_{bs}]\{U^b\} \quad (5)$$

The displacement vectors with respect to fixed axes for the body and bogies are respectively

$$\{U^c\} = [\bar{y}\ \bar{\theta}\ \bar{\alpha}]^T; \{U_k^b\} = [y_k\ \theta_k\ \alpha_k]^T \quad (6a, b)$$

In witch $[\ ]^T$ indicates transposed matrix

$\{\bar{U}_k\}$ are vectors representing the relative displacements in the x, y and z direction springs between the body and the bogies.

In equations (5) $[T_c]$ and $[T_{bs}]$ are the transfer matrices:

$$[T_c] = \begin{bmatrix} 0 & 0 & -\bar{d}(-1)^{j+1} \\ 1 & -\bar{h}_1 & \bar{A}(-1)^{k+1} + \bar{a}(-1)^{i+1} \\ 0\ \bar{d}(-1)^{j+1} & & 0 \end{bmatrix} \quad (7)$$

$$[T_{bs}] = \begin{bmatrix} 0 & 0 & -\bar{d}(-1)^{j+1} \\ 1 & -H & \bar{a}(-1)^{i+1} \\ 0\ d(-1)^{j+1} & & 0 \end{bmatrix} \quad (8)$$

Similarly, relative displacement vector between the bogies and wheel sets is

$$\{U_{ki}\} = [T_{bp}]\{U_k^b\} - [T_e]\{U_{ki}^e\} \quad (9)$$

$\{U_{ki}\}$ the vector representing the relative displacements in the x, y and z direction springs between the bogies and the wheel sets.

The displacement vector with respect to fixed axes of the wheel sets is:

$$\{U_{ki}^e\} = [y_{ki}\ \alpha_{ki}\ \varphi_{kij}]^T \quad (10)$$

$[T_{bp}]$ and $[T_e]$ transfer matrices between the bogies and the wheel sets:

$$[T_{bp}] = \begin{bmatrix} 0 & 0 & -d(-1)^{j+1} \\ 1 & -h_1 & a(-1)^{i+1} \\ 0\ d(-1)^{j+1} & & 0 \end{bmatrix} \quad (11)$$

$$[T_e] = \begin{bmatrix} 0 & -d(-1)^{j+1} & 0 \\ 1 - l\Gamma & 0 & 0 \\ d(-1)^{j+1}\ \Gamma & 0 & 0 \end{bmatrix} \quad (12)$$

Denoting the potential energy by V, we have:

$$V = \frac{1}{2}\sum_{k=1}^{2}\sum_{i=1}^{2}\sum_{j=1}^{2}\left[\{\bar{U}_k\}^T[K_s]\{\bar{U}_k\} + \{U_{ki}\}^T[K_p]\{U_{ki}\}\right] \quad (13)$$

Where $[K_s]$ and $[K_p]$ are the spring stiffness matrices for the secondary and primary suspension systems:

$$[K_s] = \begin{bmatrix} \bar{K}_{xk} & & \\ & \bar{K}_{yk} & \\ & & \bar{K}_{zk} \end{bmatrix}; [K_p] = \begin{bmatrix} K_{xk} & & \\ & K_{yk} & \\ & & K_{zk} \end{bmatrix} \quad (14a, b)$$

Similarly, the kinetic energy E of the entire system is:

$$E = \frac{1}{2}\{\dot{U}^c\}^T[M_c]\{\dot{U}^c\} + \frac{1}{2}\sum_{k=1}^{2}\{\dot{U}_k^b\}^T[M_b]\{\dot{U}_k^b\} +$$

$$+ \frac{1}{2}\sum_{k=1}^{2}\sum_{i=1}^{2}\sum_{j=1}^{2}\left\{\begin{matrix}\{\dot{U}_{ki}^e\}^T[M_e]\{\dot{U}_{ki}^e\} \\ + \{U_{ki}^e\}^T[C_e]\{\dot{U}_{ki}^e\}\end{matrix}\right\} \quad (15)$$

Where

$$[M_c] = \begin{bmatrix} \bar{M} & -\bar{M}h_0 & \bar{M}s_0 \\ -\bar{M}h_0 & \bar{M}\left(\bar{\Omega}_x^2 + \bar{h}_0^2\right) & -\bar{M}\bar{s}_0\bar{h}_0 - \bar{F} \\ \bar{M}s_0 & -\bar{M}\,\bar{s}_0\bar{h}_0 - \bar{F} & \bar{M}\left(\bar{\Omega}_z^2 + s_0^2\right) \end{bmatrix}; \quad (16)$$

$$\left[M_b\right]=\begin{bmatrix} M_k & -M_k h_0 & 0 \\ -M_k h_0 & M_k\left(\Omega_x^2+h_0^2\right) & 0 \\ 0 & 0 & M_k\Omega_z^2 \end{bmatrix}; \quad (17)$$

$$\left[M_e\right]=\begin{bmatrix} m_{ki}+\hat{m}_{ki}+(m_{ki}\rho_x^2+\hat{m}d'^2)\Gamma^2 & & \\ & m_{ki}\rho_z^2+\hat{m}_{ki}d'^2 & \\ & & \frac{m_{ki}}{2}\rho_y^2 \end{bmatrix}; \quad (18)$$

$$\left[C_e\right]=\begin{bmatrix} 0 & \frac{1}{2}\frac{V}{r_0}\Gamma m_{ki}\rho_y^2 & 0 \\ -\frac{1}{2}\frac{V}{r_0}\Gamma m_{ki}\rho_y^2 & 0 & 0 \\ 0 & 0 & 0 \end{bmatrix} \quad (19)$$

Relative velocity vector of displacement between body and bogies

$$\left\{\dot{U}_k^b\right\}=\left[T_c'\right]\left\{\dot{U}^c\right\}-\left[T_{bs}'\right]\left\{\dot{U}_k^b\right\} \quad (20)$$

Where (·) is the usual time derivative
With

$$\left[T_c'\right]=\begin{bmatrix} 0 & 0 & -\bar{d}(-1)^{j+1} \\ 1 & -\bar{h}_2 & \bar{A}(-1)^{k+1}+\bar{a}(-1)^{i+1} \\ 0 & \bar{d}(-1)^{j+1} & 0 \end{bmatrix} \quad (21)$$

And

$$\left[T_{bs}'\right]=\begin{bmatrix} 0 & 0 & -\bar{d}(-1)^{i+1} \\ 1 & -H_1 & \bar{a}(-1)^{i+1} \\ 0 & \bar{d}(-1)^{j+1} & 0 \end{bmatrix} \quad (22)$$

Relative velocity vector of displacement between bogies and wheel sets:

$$\left\{\dot{U}_{ki}^e\right\}=\left[T_{bp}'\right]\left\{\dot{U}_k^b\right\}-\left[T_e'\right]\left\{\dot{U}_{ki}^e\right\} \quad (23)$$

With

$$\left[T_{bp}'\right]=\begin{bmatrix} 0 & 0 & -\bar{d}(-1)^{j+1} \\ 1 & 0 & 0 \\ 0 & d(-1)^{j+1} & 0 \end{bmatrix} \quad (24)$$

And

$$\left[T_e'\right]=\begin{bmatrix} 0 & -d(-1)^{j+1} & 0 \\ 1-(h+l)\Gamma & -a(-1)^{i+1} & 0 \\ d(-1)^{j+1}\Gamma & 0 & 0 \end{bmatrix} \quad (25)$$

Finally, the dissipative energy of the system is given as:

$$\mathcal{D}=\frac{1}{2}\sum_{k=1}^{2}\sum_{i=1}^{2}\sum_{j=1}^{2}\begin{bmatrix} \left\{\dot{U}_k^b\right\}^T\left[C_s\right]\left\{\dot{U}_k^b\right\}+ \\ \left\{\dot{U}_{ki}^e\right\}^T\left[C_p\right]\left\{\dot{U}_{ki}^e\right\} \end{bmatrix} \quad (26)$$

Where

$[C_s]$ is the damping matrix for the secondary suspension, $[C_p]$ is the damping matrix for the primary suspension. They are given as:

$$\left[C_S\right]=\begin{bmatrix} \bar{C}_x & & \\ & \bar{C}_y & \\ & & \bar{C}_z \end{bmatrix}; \quad \left[C_p\right]=\begin{bmatrix} C_x & & \\ & C_y & \\ & & C_z \end{bmatrix} \quad (27a, b)$$

In which $\bar{C}_x, \bar{C}_y$ and $\bar{C}_z$ denote the constants of the damper units located between the bogies and body respectively in the *x*, *y* and z direction.

C_x, C_y and C_z are constants of the damper units located between the bogies and wheel sets respectively in the x, y and z direction.

Now, using the generalized displacement vector for the system

$$\{X\}=\left\{\left\{U^c\right\}^T,\left\{U_k^b\right\}^T,\left\{U_{ki}^e\right\}^T\right\}^T \quad (28)$$

And applying Lagrange's equation for each generalised coordinates, the equations of motion for the system can be written as:

$$[M]\{\ddot{X}\}+\left[D'\right]\{\dot{X}\}+\left[K'\right]\{X\}=\begin{bmatrix} Q_1 \\ Q_2 \\ Q_3 \end{bmatrix} \quad (29)$$

Where [*M*], [*D*'] and [*K*'] are respectively the inertia matrix, the damping matrix and stiffness matrix

where $\{Q_1\}=\left[K_{cg}\right]\left\{U^c\right\}$; $\{Q_2\}=\left[K_{bg}\right]\left\{U^b\right\}$ (30a, b)

$\left[K_{cg}\right]$ And $\left[K_{bg}\right]$ matrices being below on the gravity effect, respectively, for the body and the bogies

$$\left[K_{cg}\right]=\begin{bmatrix} 0 & \bar{M}gh_0 & 0 \\ 0 & 0 & 0 \\ 0 & 0 & 0 \end{bmatrix}; \left[K_{bg}\right]=\sum_{k=1}^{2}\begin{bmatrix} 0 & M_k g h_0 & 0 \\ 0 & 0 & 0 \\ 0 & 0 & 0 \end{bmatrix} \quad (31a, b)$$

$\{Q_3\}$ is a vector with twelve components representing the generalised forces acting between wheels and rails and in the torsional damper.

$$\left\{Q_3\right\}=\left[K_{eg}\right]\left\{U_{ki}^{e'}\right\}+[C]\left\{\dot{U}_{ki}^{e'}\right\} \quad (32)$$

Where $\left\{U_{ki}^{e'}\right\}=\left\{y_{ki}\ \alpha_{ki}\ \bar{\varphi}_{ki}\right\}$ and $\bar{\varphi}_{ki}=\varphi_{ki1}-\varphi_{ki2}$ (33a, b)

Where $\left[K_{eg}\right]$ and [*C*] are matrices including the effect of gravity and the creep forces

$$\left[K_{eg}\right]=\begin{bmatrix} k_g & & \\ & k_g & \\ & & k_g \end{bmatrix}; [C]=\begin{bmatrix} c' & & & \\ & c' & & \\ & & c' & \\ & & & c' \end{bmatrix} \quad (34a, b)$$

With

$$[k_g]=\begin{bmatrix} -2C_{23}\chi\frac{\gamma_0}{r_0}\left(\frac{\gamma_0}{r_0}-\frac{1}{\gamma_0 R}\right)-Wg\xi & 2C_{22}\chi & 0 \\ -2C_{33}\frac{\gamma_e}{r_0}\left(\frac{\gamma_0}{r_0}-\frac{1}{\gamma_0 R}\right) & -2C_{33}+Wg\varepsilon_0\gamma_0 & 0 \\ -2\frac{\gamma_e}{r_0}\left(-2\frac{V}{r_0}C_\varphi+\frac{C_{33}}{R}-C_{33}\frac{\gamma_0^2}{r_0}\right) & 2C_{23}\gamma_0 & 0 \end{bmatrix} \quad (35)$$

$$[C'] = \begin{bmatrix} -2C_{22}\frac{\chi^2}{V} & -2C_{33}\frac{\chi}{V}\left(1+\frac{e_0\gamma_0}{r_0}\right) & C_{23}\chi\frac{\gamma_0}{V} \\ 2C_{23}\frac{\chi}{V} & -2C_{33}\frac{1}{V}\left(1+\frac{e_0\gamma_0}{r_0}\right) & -C_{11}\frac{e_0 r_0}{V}+C_{33}\frac{\gamma_0}{V} \\ -2C_{23}\chi\frac{\gamma_0}{V} & 4C_\varphi\frac{e_0}{\gamma_0}+2C_{33}\frac{\gamma_0}{V}\left(1+\frac{e_0\gamma_0}{r_0}\right) & -2C_\varphi - C_{11}\frac{r_0^2}{V}+C_{33}\frac{\gamma_0^2}{V} \end{bmatrix} \quad (36)$$

In which
C_{11}, C_{22} and C_{23}, C_{33} are the creep and spin coefficients. They are functions of the elastic properties (Young's modulus E=2.10 10^{11} N.m^{-2}, Poisson's ratio 0.25) of the wheels and rail and of the area of contact. The creep theory was analysed by Kalker [10, 11] who was defining a digital process for the evaluation of the contact forces acting on the wheels.

$$W = \frac{\bar{M}}{4}+\frac{M}{2}+m+\hat{m} \quad (37)$$

$$\chi = \frac{e_0}{e_0 - r_0\gamma_0} \quad (38)$$

$$\gamma_e = \frac{R\,\gamma_0}{R-R'}\left[\frac{e_0+R'\gamma_0}{e_0 - r_0\,\gamma_0}\right] \approx \frac{R\,\gamma_0}{R-R'} \quad (39)$$

The gained experience testifies to the fact that the change of R' is smaller as compared with the change or R during the wear adaptation period. Therefore, the effective conicity can be viewed as a measure of the wear of the wheels.

Remarks on the transverse dynamic

It is also natural to describe the behaviour of the vehicle by the lateral movement of the body ends $\bar{y}_1$ and $\bar{y}_2$. These points belonging to the body are in the vertical passing through the gravity centres of solid C_1 and C_2. On the other hand, this identification is available to the measure. It is easy to write the relations of liaison:

$$\bar{y} = \frac{\bar{y}_1+\bar{y}_2}{2} \text{ et } \bar{\alpha} = \frac{\bar{y}_1-\bar{y}_2}{2\,\bar{A}} \quad (40a, b)$$

The development of calculations that we do not reproduce shows that the variables $\bar{y}_1$ and $\bar{y}_2$ are decoupled and the system simplified provided to affect to each solid C_1 and C_2 the suspended half mass of the body. Finally, the model consists of two wheel sets, a bogie and a half body.
Therefore, the vehicle has 13 degrees of freedom. The notation adopted (33b) reduce the differential system to 11 equations given in [12] with two springs instead of four in the secondary suspension.

4.4 Resolution

Substituting equations (1), (30a, b) and (32) into equation (29), we obtain the linear differential equations with constant coefficients of the form:

$$[M]\{\ddot{q}_i\}+[D]\{\dot{q}_i\}+[K]\{q_i\}=\{0\} \quad (41)$$

Where
[M] Is the matrix of inertia
[D] is damping matrix function of: the speed of movement, the suspension parameters and the parameters relative to the geometry of contact.
[K] is the matrix stiffness depending on: the speed of movement because of the torsional damper, the suspension parameters and the parameters relative to the geometry of contact.
$\{\ddot{q}_i\}$ is the accelerations vector ;
$\{\dot{q}_i\}$ is the velocity vector ;
$\{q_i\}$ is the displacements vector .

Equation (41) represents a set of 11-second order homogeneous equations with non-proportional damping. Each component of eigenvector is distinguished not only by amplitude but also by phase angle. Thus, 22 equations are required to determine all components of the system with 11degree of freedom. Therefore, in addition to the 11 equations of motion, another 11 equations are needed to obtain a system of 22 equations. We use a method suggested by Duncan-Frazer. These 11 additional equations are given by the following matrix identity:

$$[M]\{\ddot{q}_i\} - [M]\{\dot{q}_i\} = \{0\} \quad (42)$$

Equations (40) and (41) can be combined to give the following matrix equation:

$$\left[\begin{array}{c|c} [M] & [0] \\ \hline [0] & [I] \end{array}\right]\left\{\begin{matrix}\ddot{q}_i \\ \dot{q}_i\end{matrix}\right\}+\left[\begin{array}{c|c} [D] & [I] \\ \hline -[I] & [0] \end{array}\right]\left\{\begin{matrix}\dot{q}_i \\ q\end{matrix}\right\}=\{0\} \quad (43)$$

Where [I] is the identity matrix
Equation (42) can be written as:

$$\left[M^*\right]\left\{\begin{matrix}\ddot{q}_i \\ \dot{q}_i\end{matrix}\right\}+\left[K^*\right]\left\{\begin{matrix}\dot{q}_i \\ q\end{matrix}\right\}=\{0\} \quad (44)$$

Let

$$\{x(t)\}=\left\{\begin{matrix}\dot{q}_i(t) \\ q(t)\end{matrix}\right\} \quad (45)$$

Then

$$\left[M^*\right]\{\dot{x}(t)\}+\left[K^*\right]\{x(t)\}=\{0\} \quad (46)$$

Let

$$\{x(t)\}=e^{pt}\{x\} \quad (47)$$

Then

$$p\left[M^*\right]\{x\}+\left[K^*\right]\{x\}=\{0\} \quad (48)$$

Of such form:

$$[A]\{x\}=p\{x\} \quad (49)$$

With

$$[A]=-\left[M^*\right]^{-1}\left[K^*\right]=\left[\begin{array}{c|c} -[M]^{-1}[D] & [M]^{-1}[K] \\ \hline [I] & [0] \end{array}\right] \quad (50)$$

Equation (49) is the standard form of the eigenvalue problem and leads to a set of 22 eigenvalues. For a stable system, each of these eigenvalues $p=\alpha+j\omega$ will be either real and negative or complex with a negative real part: $\alpha < 0$. If the eigenvalues are complex, they will

occur in conjugate complex pairs. The transition from the case $\alpha < 0$ to the case $\alpha > 0$ corresponds to the modes:

- $\alpha = 0$; $\omega \neq 0$: zero damped, steady oscillations i.e., those continually repeated (self-excited) which are especially dangerous.
- $\alpha = 0$; $\omega = 0$: so called rigid-mode, constant momentum.

The eigenvalues were computed by the Q-R double step method.

5. RESULTS AND DISCUSSIONS

5.1 Effect of primary suspension

Figure-2 shows the critical speed beyond which the vehicle is unstable for different effective conicities begining with γ_e =0.1 until 0.3. The curve is obtained for damping coefficient value C_φ = .5 MN.m.s.rad^{-1}.

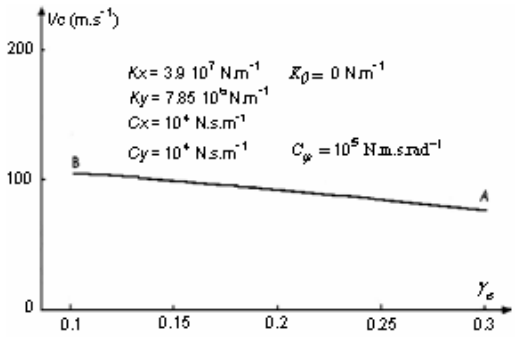

Figure-2. Critical speed *Vc* versus effective conicity γ_e and a particular value of *Kx*, *Ky*, *Cx* and *Cy*.

The same curve was obtained in [2] for a classic vehicle with the same characteristics of construction given in the nomenclature. We can see that a great effective conicity has a destabilizing effect. The value of C_φ imposes a highest constraint on the wheels, that is, each wheel set seems to be a single piece. The longitudinal stiffness is too high. It is practically impossible to change it during motion.

Figure-3 gives the critical speed depending on the effective conicity for two values of damping $C_{\varphi 1}$ between the wheels of the leading wheel set.

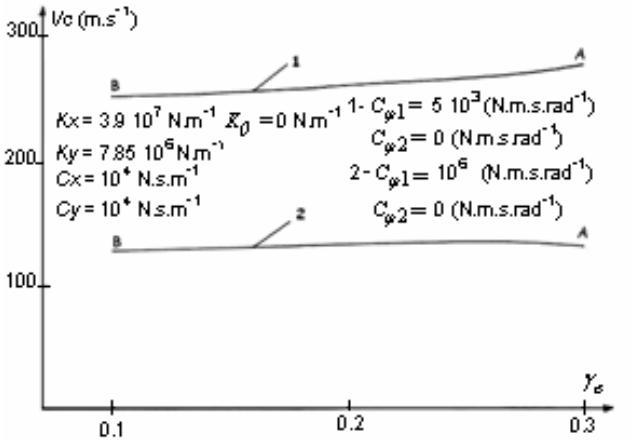

Figure-3. Variation of a critical speed versus γ_e for 2 values of $C\varphi_1$; $C\varphi_2$=0 N.m.s.rad^{-1}

The wheels of the trailing wheel set remain free, that is, the coefficient $C_{\varphi 2}$ is nil. It can be seen that the critical speed is becoming higher with the decrease in $C_{\varphi 1}$. A remarkable fact, the curve 1 is increasing with the decrease in $C_{\varphi 1}$. In contrast, the curve 2 and the previous curve in Figure-2 show a decrease in critical speed. The possibility of constructing a vehicle running faster on an increasingly worn path is open. However, we cannot avoid flange contact and wear of the trailing wheel set, particularly in the rail-curved tract. Such a vehicle is less expedient in that it does not preclude the flange contact. Let us not negate the risk of climbing. The high speed augments the skidding hazard.

Here after, we will meet one of the points raised in the foreword. What happens to the area of stability for a softer longitudinal stiffness? The answer to this question is shown in Figure-4.

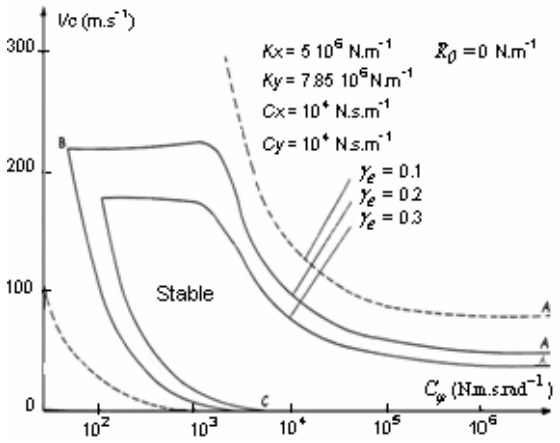

Figure-4. Dependence of the critical speed on C_φ for 3 values of γ_e and a particular value of *Kx, Ky, Cx* and *Cy*.

Three curves define the limits stability for *Kx* = 5.0 MN.m^{-1}. It provides the critical speed depending on the coefficient C_φ the same for both wheel sets. The curves circumscribe an area as representation of vehicle stability for three values of the effective conicity. Strong effective conicity and greater damping in rotation between the wheels have the effect of reducing the area of stability. This fact result from the increase of the first critical speed (CB branch; unspecified in the previous figures, because this first critical speed is small $Vc \approx 0.5$m.s^{-1}). Below that speed, the vehicle is unstable; its temporal evolution is divergent, that is, the mode motion is: Statically unstable nonoscillatory, exponential growth. Above that speed, we cross a zone of stability until the ultimate speed or second critical speed (branch *AB*) is reached where the vehicle is unstable once more. The temporal evolution is divergent with oscillations, that is, the mode motion is: Negatively damped, sinusoidal, exponential growth. It notes that the increased guidance that we could expect with the increase in the effective conicity reduces the second critical speed. Despite this deterioration, even with a strong effective conicity (curve 3) where the intersection of the two branches arrive sooner, the critical speed is 178m.s^{-1} for C_φ =.0015 MN.m.s.rad^{-1}. This value is well above the current traffic speeds allowed with *Kx*=39 MN.m^{-1}. All thing being equal, it is well above the conventional vehicle speed limit. From this Figure, the pre-assigned value of C_φ =.0015 MN.m.s.rad^{-1} preserves the stability motion even with the wheel tread completely worn out. Moreover, high conicity improves curving performance [1].

For this stiffness *Kx*=39MN.m^{-1}, 3 values of γ_e and different values of C_φ, we obtain the results of Figure-5.

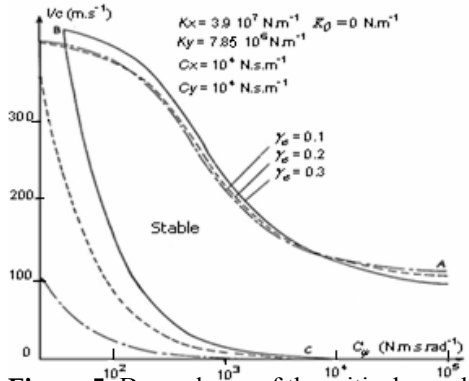

Figure-5. Dependence of the critical speed on C_φ for 3 values of γ_e and a particular value of *Kx*, *Ky*, *Cx* and *Cy*.

We deduce from these performances curves that the first critical speed becomes embarrassing for $C_\varphi \leq 10^3$ N.m.s.rad^{-1}. C_φ =.005 MN.m.s.rad^{-1} and *Vc* =130m.s^{-1} are the ordinate of a common point relative to the three branches of the second critical movement. The critical speed is independent from the value of γ_e.The effective conicity has an adverse effect beyond this common point. The critical speed diminishes as γ_e is increased for C_φ

>.005 MN.m.s.rad^{-1}. If C_φ is lower, the reverse dependence is observed, i.e. the critical speed will increase as γ_e increases:

-Once more, the wheel tread wear does not impair the stability; besides, the vehicle is more stable.

-The high value of rigidity illustrated in the figure may allow the designer to dispense with elastic element in the primary suspension.

-The critical speeds are frankly too high. There is no mind to reduce the high margin of safety against the onset of vibration by using a smaller wheelbase, which promotes good curving performance [1].

These results demonstrate that the wheels with controlled creep forces give an opportunity to design a stable vehicle at high speeds. There is no need for a high value of *Kx*. The critical speed required can be obtained with a soft stiffness *Kx*. The calculation shows that it is appropriate to impose a stiffness $Kx \geq 5.0$ MN.m^{-1} and $Ky = 7.85$ MN.m^{-1} to obtain a satisfactory dynamic behaviour of the vehicle. The rigidity being low, it should be interesting to use the pneumatic elastic elements. The rigidity of a pneumatic suspension can be changed easily within wide limits.

This stiffness Kx=5.0 MN.m^{-1} led to a satisfactory behaviour in the curved tract. We must enslave the damping effect between wheels at the desired speed of the vehicle so to exceed the speed practiced today. The key is to increase the resistance coefficient according the stability results as curvature increases. The main purpose of adjustable coupling in rotation between wheels is to make the vehicle travelling as fast as possible round a curve of a definite radius and a defined cant without skidding. The torsional damper allows us to suit the conditions of motion and avoids us to drop the speed drastically as for a conventional vehicle [12].

We deduce from these results, that the free wheels system is unacceptable. The vehicle is inherently unstable for C_φ equal to zero. The torsional damper appears as a security organ. In addition, with the free wheels, no wheel prevents the other from rotation; as a result, we lose the guidance inherent in conical wheels.

5.1.1 Longitudinal damping effect *Cx*

Calculations show that the first critical speed is not affected by the parameter *Cx*. For stiffness Kx= 50.0 MN.m^{-1}, the action in the longitudinal direction plays no role. For *Kx* values ranging from .1 to 1.0 MN.m^{-1}, we see that it is interesting to complete the stiffness with a damper and particularly for $C_\varphi < 10^4$ N.m.s.rad^{-1}. For stiffness of interest from Kx=5.0 MN.m^{-1} to Kx=10.0 MN.m^{-1} and for C_φ <1600 N.m.s.rad^{-1} there is an appreciable increase in the second critical speed.

5.1.2 Transverse damping effect *Cy*

The stabilizing effect appears only for $Ky \leq 1.0$ MN.m^{-1} and Kx>10.0 MN.m^{-1}. For lowest values of *Kx* the transverse damping help to obtain more stability for $C_\varphi < 10^3$ N.m.s.rad^{-1}. The first critical speed is unchanged.

5.1.3 Transverse stiffness effect *Ky*

There are no changes in the first critical speed related to the *Ky* stiffness. With high *Ky* stiffness, the instability on the second critical movement appears at higher speeds. However, the transverse stiffness must be chosen according to the stiffness *Kx*.

5.1. Longitudinal stiffness effect *Kx*

The fist critical speed is somewhat influenced by the *Kx* stiffness. Instability moves at slightly speeds with the increase of the latter. There is a substantial increase in the critical speed in the second critical movement for C_φ<1600 N.m.s.rad^{-1}. Thus, we produce a large area of stability with large values of *Kx* stiffness.

5 2 Influence of the secondary suspension

The parameters relating to the secondary suspension should be low to prevent the bogies movement transmission to the body.

5.2.1 Influence of stiffness $\bar{K}_0$

Figure-6 shows speed variations beyond which the vehicle undertakes instability for different effective conicities and two $\bar{K}_0$ values. These results were obtained for C_φ =.5 MN.m.rad^{-1}.

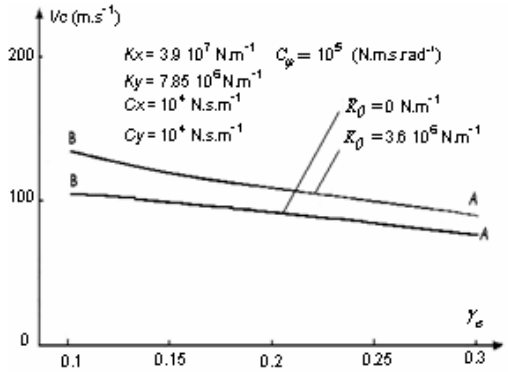

Figure-6. Variation of the critical speed with γ_e for 2 values of $\bar{K}_0$ and a particular value of *Kx*, *Ky*, *Cx* and *Cy*.

The same results were obtained in [2] for a classic vehicle. The secondary anti-yaw constraint leads to a substantial increase of the second critical speed. The first critical speed referring to a static instability unrepresented is about 0.5m.s^{-1}.

The curve on Figures-7 and 8 for $\bar{K}_0$=0 can be compared with the corresponding curve for $\bar{K}_0$=3.6 MN.m^{-1} of the Figures respectively 9 and 10.

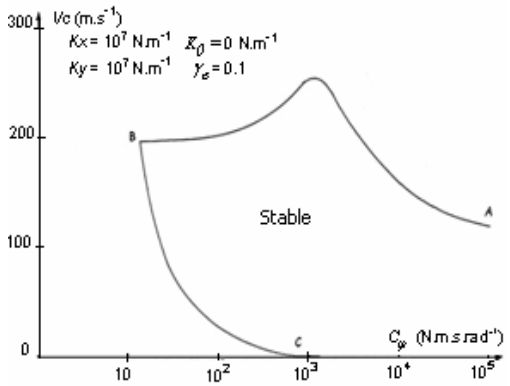

Figure-7. Variation of the critical speed with C_φ for $\bar{K}_0 = 0$ N.m^{-1}, $\gamma_e = 0.1$and a particular value of *Kx*, *Ky*, *Cx* and *Cy*.

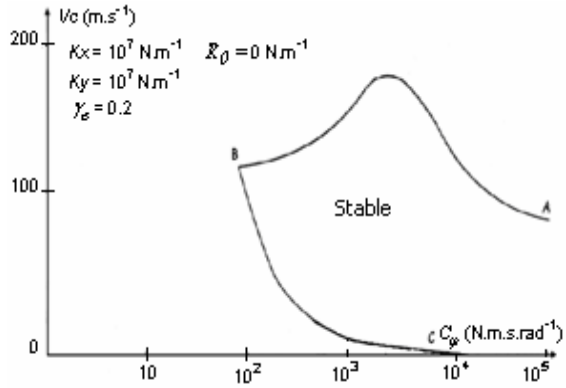

Figure-8. Variation of the critical speed with C_φ for $\bar{K}_0 = 0$ N.m^{-1}; $\gamma_e = 0.2$ and a particular value of *Kx*, *Ky*, *Cx* and *Cy*.

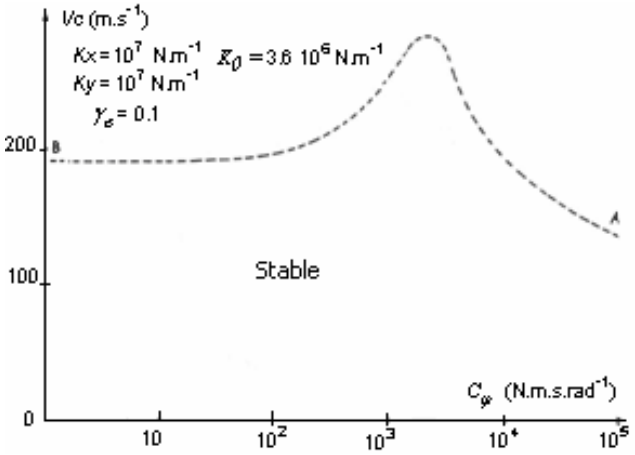

Figure-9. Variation of the critical speed on C_φ for $\bar{K}_0 \neq 0$ N.m^{-1}; γ_e = 0.1and a particular value of *Kx*, *Ky*, *Cx* and *Cy* (to compare with Figure-7).

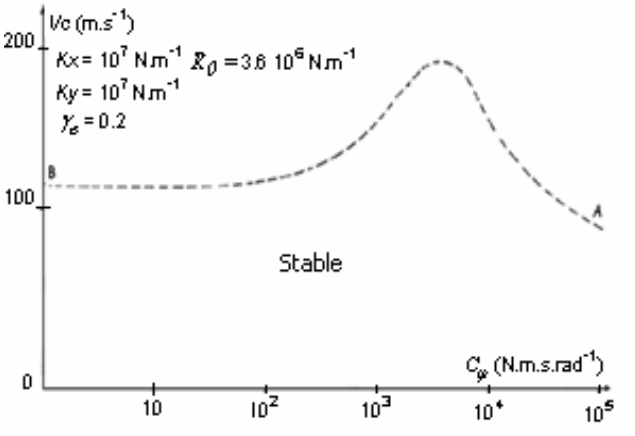

Figure-10. Variation of the critical speed with C_φ for $\bar{K}_0 \neq 0$ N.m^{-1}; γ_e = 0.2and a particular value of *Kx*, *Ky*, *Cx* and *Cy* (to compare with Figure-9).

We show the positive effect of the anti-yaw constraint $C(\alpha) = 2\bar{K}_0\bar{b}_0^2\alpha$ on the limits of stability for two values of the effective conicity. The parameter *Cx* has no effect on these limits. It can be gathered from the curves a remarkable result for *Kx*=10 MN.m^{-1}: the vehicle is stable even when C_φ falls to zero. The choice of suitable parameter C_φ can largely offset the decline in the critical speed resulting from wear of treads, flanges and rail. The torsional damper is no longer a security organ.

A vehicle with free wheels inherently unstable becomes seemingly stable through stiffness, which exerts a constraint against the yaw bogie. However, as for a classic vehicle, failure of the anti-yaw damper becomes troublesome for the security. At the crossing of the curve, it is necessary to incorporate a torsional damper to maintain the wheels guidance by the creep forces. Moreover, interference from the effect of the $\bar{K}_0$ stiffness with the good traversing in curves has often been cited as a disadvantage and a limitation. The first critical speed (branch CB) is widely disparaged ($Vc \approx 0.5$m.s^{-1})

5.2.2 Transverse stiffness effect $\bar{K}_y$

For low values of C_φ, calculation shows an increase in the second critical speed due to rise of $\bar{K}_y$. The effect of this stiffness on the first critical speed is negligible.

5.2.3 Transverse damping effect $\bar{C}y$

A high $\bar{C}y$ value leads to an increase of the second critical speed. This parameter does not affect the first critical speed.

5.2.4 Stiffness influence in vertical direction

The primary vertical stiffness and the secondary ones must be chosen adequately: the desirable coupled low

frequency within recommended limits (1-1.3 Hz) and so that the high coupled frequency as far as possible from the body natural frequency.

5.3 Masses influence

The influence of the masses takes interest on the dynamics when you try to alleviate the structures either by reducing sections either by using lighter materials.

5.3.1 Body mass

This mass varies with the load conditions. The smallest mass has a stabilizing effect in spite of the gravity constraint reduction. This effect is more pronounced with highest values of *Kx*. It should be noted that the creep coefficients decreases with both the reduced mass and the reduction in the effective conicity.

5.3.2 Bogie mass

The solution shows that only the radius of inertia about the vertical axis has a great importance, and only for the second critical speed. To achieve a bogie with a given wheelbase stable at high speeds, it is important to reduce and concentrate the mass as much as possible in order to reduce the radius of inertia about the vertical axis. For this reason, the rail vehicle has the engines mounted on the under body frame.

5.3.3 Wheel set mass

Heavy wheel sets have an adverse effect on the vibration behaviour for all kind of railway vehicles. On the other hand, the calculation shows that we must minimize the radii of inertia. It is expedient to decrease the mass of this part not suspended. This reduces the load on the dampers and improves the conditions wheel sets oscillations.

6. Remarks

The calculation shows that overvaluation of the gravitational rigidity by 10 times leads to a considerable reduction of the first critical speed. The maximum is about 0.5 m .s^{-1} .There is a positive effect on the second critical speed, which is slightly affected.

The critical speeds beyond 500km.h^{-1} are only indicative values: the quasi-static theory of Kalker being no longer valid. The inertial effects become noticeable in contact theory for train speeds of over 500km.h^{-1}.

7. CONCLUSIONS

What can we learn from this study? What comes first is that the technological innovation relating to the wheel set gives us the possibility of going faster. The stability, which limits the maximum safe speed of the vehicle, is heavily dependant on the longitudinal stiffness of the primary suspension and the damping coefficient in rotation between wheels. In the new line, the so-called "TGV" can be displaced by another one, which has in everything the same characteristics unless the peculiar wheel set in design. It is possible to shorten the wheelbase for good curving performances. Therefore, the damper has an appreciable effect on the performance of the rail vehicle, all other conditions being equal, in the straight line as well as on the curved tracks. The revamping of the other rail vehicles is relevant too.

We can achieve good stability with a relatively soft stiffness *Kx*, a parameter that affects the ability of self-steering round the curves. For a relatively lower stiffness *Kx*, a moderate stiffness *Ky* and a small damping between wheels, the second critical speed is already sent outside the range of speeds routinely practised, that is, even with a worn area of contact. The damping coefficient in rotation is an important design parameter, making it to vary the critical speed. The torsional damper requires adjustment or servicing to insure the maximum possible speed in the curved tracks. This means that the vehicle accommodates existing channels. It is within the reach of networks that cannot consider the construction of a new high-speed line. The importance of the connections between body and bogies is less crucial. The vehicle behaviour remains satisfactory with a soft secondary suspension. Only the $\bar{K}_0$ stiffness has a significant influence on the two critical speeds with this beneficial fact: the failure of the torsional damper no more compromising the security for a moderate stiffness *Kx* = 10.0 MN.m^{-1}.

We note also that large wheel set masse have a destabilising effect as for a classic vehicle, but unlike the latter higher speeds are possible through an appropriate damping between wheels.

REFERENCES

[1] D. Boocock. 1969. Steady-state motion of railway vehicles on curved tract, Journal Mechanical Engineering Science. Vol. n° 6.

[2] R. Joly. 1983. Stabilité transversale et confort vibratoire en dynamique ferroviaire, Thèse de doctorat d'Etat, Université de Paris VI.

[3] J-P. Chenais, L. Hazard, G. palais. 2000. Amélioration du confort dynamique des trains dans l'optique d'une augmentation des vitesses, Mécanique and Industries. 1,123-130

[4] M. G. Pollard. 1985. Le développement de bogies croisillonnés pour wagons de marchandises, Rail International nov. N° 11,

[5] H. Scheffel. 1974. Stabilisation du mouvement de galop et facilité d'inscription des véhicules ferroviaires dans les courbes. Rail International, Mars.

[6] P. Becker. 1970. A propos du problème des roues indépendantes sur véhicules ferroviaires, Einsenbahn Technische Rundschau nov.

[7] F. Frederich. 1985. Possibilités inconnues ET inutilisées du contact Rail/Roue-Rail International nov. N° 11.

[8] C. K. Benington. 1968. The railway wheelset and suspension unit as closed-loop guidance system: method for performance improvement, Journal Mechanical Engineering Service. Vol. n°2.

[9] A.D. Pater. 1963. Précis de la théorie de l'interaction entre la voie et le véhicule du chemin de fer. Document ORE UTRCHT.

[10] J. J. Kalker. 1967. on the rolling contact of two elastic bodies in the presence of dry friction, Doctorate Thesis-Delft University.

[11] J. J. Kalker. 1979. Survey of Wheel-Rail Rolling Contact Theory, Vehicle System Dynamics. 5. pp. 317-358.

[12] M. Messouci. 1987. Performances d'un véhicule ferroviaire muni de roues à pseudo glissement contrôlé, stabilité transversale en alignement et inscription en courbe, Thèse, ENSAM. Paris.

Notations and parameters for example vehicle		
$2\overline{A}$	distance between bogies centres	18.135 m
$2\overline{a}$	longitudinal distance of the springs and dampers	2 m
$2a$	wheelbase of bogie	3 m
$\overline{b}_0$	distance between the anti-yaw body/bogie device levers	1.3 m
$4Cx$	longitudinal damping coefficient of the primary suspension	variable
$4Cy$	transversal damping coefficient of the primary suspension	variable
$4\overline{Cx}$	longitudinal damping coefficient of the secondary suspension	0 N.s.m^{-1}
$4\overline{Cy}$	lateral damping coefficient of the secondary suspension	4x.035 MN.s.m^{-1}
$\overline{Cz}$	vertical damping coefficient of the secondary suspension	.015 MN.s.m^{-1}
$C\varphi$	coefficient of resistance or damping between wheels of a wheel set	variable
$2d$	transverse distance of the springs and dampers for the primary suspension	2 m
$2\overline{d}$	transverse distance of the springs and dampers for the secondary suspension	2 m
$2d'$	transverse distance between inertia centres of wheels bearings box *(~ 2 d)*	
$2e_0$	semi-track of wheel set	1.5 m
g	gravitational acceleration	9.81 m.s^{-2}
$\overline{h}_0$	position of secondary plane of suspension relative to $\overline{G}$	0.880 m
$\overline{h}_1$	half height of the secondary suspension	0.210 m
$\overline{h}_2$	transverse damper position in the secondary suspension relative to secondary plan of suspension	0 m
h_0	position of primary plane of suspension relative to G_k	.120 m
h_1	half height of the primary suspension	0 m
H	vertical distance between springs points attachments of secondary suspension relative to the primary plane of suspension	0,467 m
H_1	vertical distance between transverse dampers of secondary suspension relative to the primary plane of suspension	0.670 m
H_p	distance between the lower operative point in bogie frame of the training device with the primary transverse plane of suspension	
$4Kx$	longitudinal stiffness of the primary suspension	variable
$4Ky$	transversal stiffness of the primary suspension	variable
$4Kz$	vertical stiffness of the primary suspension	4 x.975 MN.m^{-1}
$4\overline{Kx}$	longitudinal stiffness of the secondary suspension	4 x .175 MN.m^{-1}
$4\overline{Ky}$	transversal stiffness of the secondary suspension	4 x.173 MN.m^{-1}
$4\overline{Kz}$	vertical stiffness of the secondary suspension	4 x .53 MN.m^{-1}
$\overline{K}_o$	levers stiffness of anti -yaw device between body and bogie	3.6 MN.m^{-1}
$2l$	wheel- axle set diameter	0.165 m
m	mass of a wheel set	1500 kg
$\overline{m}$	mass of a wheel set box or journal bearing	250 kg
$\overline{M}$	mass of a body	43200 kg
M	mass of a bogie	3020 kg
R'	curvature radius of a rail profile	0,30 m
R	curvature radius of wheel profiles	function of γ_e
r_o	mean radius of wheel	0.45 m
s_o	longitudinal eccentricity of $\overline{G}$	0.1 m
V	vehicle speed	m.s^{-1}
V_c	critical speed	m.s^{-1}
γ_0	angle of the tangential plane to the common points of contact wheel/rail with the horizontal plane when the wheel set is centred in	0.025

	the midline of the rail	
γ_e	effective conicity	
ρ_x	radius of inertia of the wheel set around $G_{ki}\, x_{ki}$ axis	0.73 m
ρ_z	radius of inertia of the wheel set around $G_{ki}\, z_{ki}$ axis	0.73 m
ρ_y	radius of inertia of the wheel set around $G_{ki}\, y_{ki}$ axis	0.25 m
φ_{kij}	increment in the angle of rotation around the axis of the wheel S_{kij} relatively to an imaginary wheel coinciding with the latter and rolling without slipping	
$\bar{\Omega}_y$	radius of inertia of the body about $\bar{G}y$ axis	7.50 m
$\bar{\Omega}_x$	radius of inertia of the body about $\bar{G}x$ axis	1.27 m
$\bar{\Omega}_z$	radius of inertia of the body about $\bar{G}z$ axis	7.50 m
Ω_x	radius of inertia of the bogie about $G_k\, x_k$ axis	0.84 m
Ω_y	radius of inertia of the bogie about $G_k\, y_k$ axis	1.16 m
Ω_z	radius of inertia of the bogie about $G_k\, z_k$ axis	1.16 m

The inertia matrix of the body (*C)* attached to (***x, y, z***) coordinates system in $\bar{G}$ is:

$$I\left(\bar{G},C\right)=\begin{pmatrix} \bar{M}\Omega_x^2 & 0 & -\bar{F} \\ 0 & \bar{M}\Omega_y^2 & 0 \\ -\bar{F} & 0 & \bar{M}\Omega_z^2 \end{pmatrix}_{x,y,z}$$

Subscripts

k (k = 1 for the leading truck and k = 2 for the trailing truck).
i (i = 1 for the leading wheel set of a truck and i = 2 for the trailing wheel set of a truck).
j (j = 1 for the left hand side and j = 2 for the right hand side).